Terahertz Channel Modeling Considering Near-to-Far Field Transition: Benefits & Challenges

Priyangshu Sen*, Sherif Badran†, Josep M. Jornet†, and Arjun Singh*
*Department of Engineering, SUNY Polytechnic Institute, Utica, NY 13502, USA
†Department of Electrical and Computer Engineering, Northeastern University, Boston, MA 02115, USA
E-mail: {senp, singha8}@sunypoly.edu*, {badran.s, j.jornet}@northeastern.edu†

***Abstract*—Terahertz band (0.1–10 THz) communication is set to play a pivotal role in the advancement of subsequent generations of wireless technology by facilitating high data rates, ultra-secure transmission, high-resolution sensing, and low-latency links, among others. Nevertheless, the issues of low transmission power and high path loss necessitate large-aperture high-gain antennas, which can result in a considerably expanded near-field operational region. The distinctive mechanism of wave propagation within this region, as well as its transition to the far-field area, necessitates a comprehensive reevaluation of channel modeling. In this paper, we discuss the effects of antennas on path loss models and channel metrics while operating in both the near- and far-field regions. We present a detailed analysis of near-field propagation mechanisms, illustrating that an antenna-agnostic channel model is not feasible. Furthermore, we discuss the potential benefits and challenges associated with these regions.**

***Index Terms*—Terahertz wireless communications, channel sounding, channel modeling, near field, far field, antennas.**

I. Introduction

Terahertz (THz) band communication (0.1–10 THz) is expected to be a key technology enabling a wide range of emerging features and applications for next-generation wireless communications. These include, the provision of very high data rates for backhaul and indoor wireless access, the facilitation of high-resolution imaging and sensing, and the establishment of ultra-secure networks [1]. Recent rapid advancements in device technology [2] have led to the narrowing of the so-called THz band gap, thereby enhancing our ability to fully exploit the potential of the THz band.

Significant effort has been dedicated to theoretical studies of the propagation characteristics of THz waves [3], and point-to-point communication links have also been demonstrated experimentally [4]. Further, numerous studies have been undertaken to comprehend the THz-specific channel within both indoor [5] and outdoor [6] environments under varying weather conditions, as well as in various application-specific scenarios, including the channel for kiosk downloads [7], AR/VR applications [8], and conference room setups [9].

The significance of these (and more) previous studies is self-evident. At the same time, we highlight that these experimental studies primarily utilize a fixed antenna setup for channel measurement, which does not allow us to capture the effect of the antenna on the channel statistics. However, our study [10] has shown that the antenna not only significantly affects path loss but also influences the multipath profile (MP) and, consequently, channel metrics. This becomes even more relevant in the case of large antennas (i.e., high gain). A prime reason is due to the significant near-field distance, wherein the propagation mechanisms cannot be studied via the commonly utilized Friis path loss [11]. We highlight in [10] that achieving a channel model that is agnostic from the antenna configuration (as is commonly the case) [12] is particularly unattainable.

Understanding the channel considering the near-to-far field transition is important, as it can result in a significant deviation between expected and observed outcomes, even in straightforward line-of-sight (LoS) scenarios. This understanding becomes particularly critical in the context of mobile nodes. The significance of this understanding is further emphasized in [13], where it is mathematically demonstrated that mobile THz communications nodes must operate within the near field. Therefore, we arrive to a crucial observation: *To advance 6G and beyond, the development methodology for sub-THz and THz radio channel models must be thoroughly assessed.*

In this paper, we focus on the following major points that are crucial to consider for THz-band channel modeling. i) Antenna-centric effects in the THz channel model considering the transition from the near to the far field. ii) The subsequent path loss model, as well as the MP and channel metrics such as K-factor, delay spread, and angular spread. iii) The benefits and challenges associated with THz radios operating in a dynamic propagation environment.

The paper is organized as follows. In Sec. II, the signal propagation mechanism and beam characteristics are explained, with particular consideration given to the transition from near-to-far field and the deployment of different antennas at the transceiver. In Sec. III, we discuss the effect of this transition on the path loss model, and in Sec. IV, we delve into its impact on the MP and crucial channel metrics. In Sec. V, we provide an overview of the benefits and challenges associated with THz nodes operating in the near and far fields of the antenna. Finally, Sec. VI concludes our work.

II. Near-to-Far Field Transition

To develop a detailed understanding of the channel and the mechanisms of path loss (PL), we thoroughly explore the principles of wave propagation in both near- and far-field regions. This is particularly crucial in the case of THz frequencies,

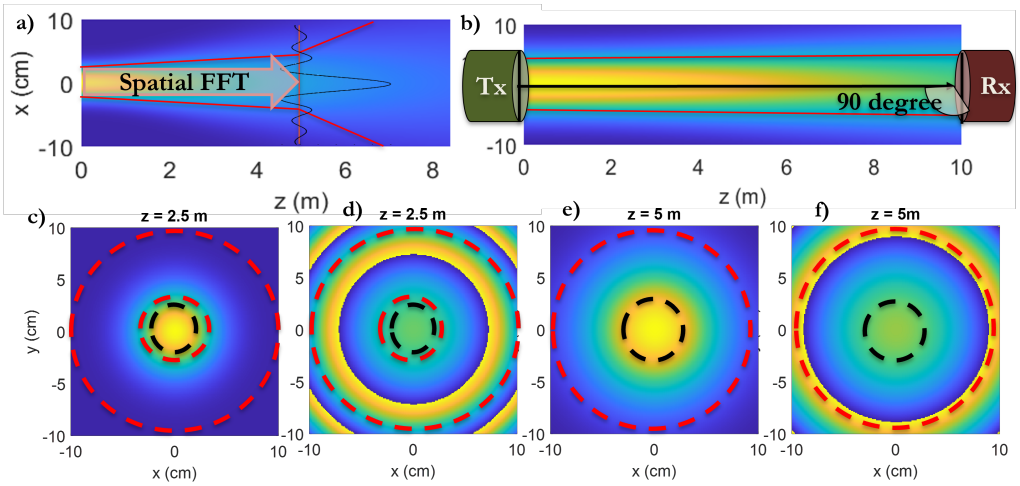

Fig. 1. Near-to-far field transition of a) a 5 cm and b) 10 cm aperture antennas at 300 GHz. c) Amplitude and d) phase profiles of a transmitter antenna ($D = 5$ cm) in the near field (2.5 m). Further, e) amplitude and f) phase profiles of a transmitter antenna ($D = 5$ cm) in the far field (5 m). The red and black circles represent the receiver aperture in the near and far fields, respectively.

as the extent of the near field is substantially greater than that of lower frequencies. For instance, at 140 GHz with a 10 cm antenna, the near-field range is 9 m; at 1 THz, it is 66 m. This indicates a potential near-to-far field transition is possible, especially for mobile nodes [13].

Near Field: The near-field region is divided into the reactive and radiative regions. In our discussion, we mainly focus on the radiative part as the reactive part is extremely short, i.e., a region where the waves are not yet decoupled from the antenna. The extent of the radiative part is given by the Fraunhofer distance [14]: $d_F = 2D^2/\lambda$, where D is the largest dimension of the antenna and λ is the wavelength. This distance increases with an increase in antenna size/gain. For example, at 300 GHz, with antenna apertures of 5 cm and 10 cm, the far fields are 5 m and 20 m, respectively. In this region, the dimensions and phase arrangement of the array or antenna (with axicons) could generate various sophisticated beam types [15], which are beyond this paper's scope. Here, we focus on the Gaussian beam [15] to explain the propagation mechanism, as it is equivalent to beamforming in the far-field region. A Gaussian beam originating with initial electric field E_0 with beam waist w_0 (aperture size $D = 2w_0$) produces the field $E(z)$ along z-axis given by [16]:

$$E(z) = E_0 \frac{w_0}{w(z)} e^{\left(\frac{-r^2}{w(z)^2} e^{\left(-j\left(kz + k\frac{r^2}{2R(z)} + \phi(z)\right)\right)} \right)}, \quad (1)$$

$$\text{where} \quad w(z) = w_0 \sqrt{1 + \left(\frac{z}{z_R}\right)^2}, \quad R(z) = \frac{z^2 + z_R^2}{z},$$

whereas $w(z)$ is the beam waist after propagating a distance z, $R(z)$ is the radius of curvature with $\phi(z) = \tan^{-1}(z/z_R)$ describing the Gouy phase, and $z_R = \pi w_0^2/\lambda$ is the Rayleigh range. The received power P_{rx} from a receiver with an aperture size w_{rx} at a link distance z is calculated as, $P_{\text{rx}} = \int_{-w_{\text{rx}}}^{w_{\text{rx}}} E(z)^2\, dr$.

It is noteworthy that the phase component $-k\frac{r^2}{2R(z)}$, where $k = 2\pi/\lambda$ is the wavenumber, varies across the cross-sectional aperture w_{rx} (Fig. 1(d)). This could create constructive or destructive sums of power at the receiver depending on the transceiver antenna size. Additionally, in close vicinity, the generated beam has the same width as the antenna aperture and can be represented approximately as a rectangular wave with an infinite radius of curvature. As it propagates, the beam gradually widens, reaching a minimum radius of curvature at the Fraunhofer distance before transitioning to the far field, signifying the maximum spread for a given antenna size/gain. In fact, a smaller antenna starts with a smaller beam waist that spreads rapidly, compared to a larger antenna, which has a larger initial beam width but spreads more slowly. The phenomenon is illustrated in Fig. 1(a) and 1(b) with 5 and 10 cm aperture antennas, respectively, at 300 GHz.

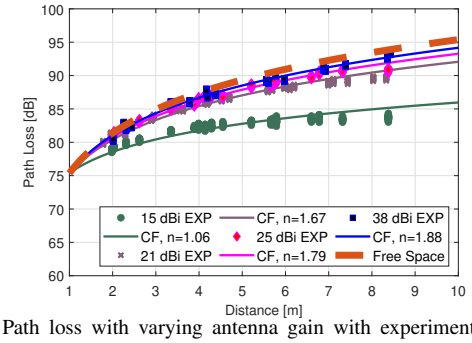

Fig. 2. Path loss with varying antenna gain with experimental (EXP) and curve fitted (CF) values.

Far Field: Upon propagating beyond the Fraunhofer distance, the beam undergoes a transition into the far-field region. It is in this region that the principles of Friis path loss and beamforming become applicable, as the parallel path or the plane wave assumption holds true [11]. Additionally, it can be demonstrated that the far and near fields are connected through the spatial Fourier transform [11]. Theoretically, it can be demonstrated that $\text{rect}(s/(2\omega_0)) \overset{\mathcal{F}}{\Leftrightarrow} 2\omega_0 \text{sinc}(\omega_0 S)$ where $2\omega_0$ is antenna aperture and s, S are spatial variables for near- and far-field waves, respectively (Fig. 1(a)). Therefore,

achieving an extremely directional narrow beam in the far field necessitates an extensive planar electric field excitation in the near field or a significantly large antenna aperture.

III. Effect on the Path Loss Model

The discussion on signal propagation reveals that an antenna-agnostic channel model is unattainable for THz frequencies [10]. The propagation mechanism and signal phase profile impinging on the receiver antenna significantly affect the path loss characteristics. Herein, we analyze the four potential scenarios that directly impact the received power and hence the path loss, considering the transition from near to far field.

a) Transceiver Antennas in Near Field: In this scenario, a broad beam, equivalent to the transmitting antenna aperture's size, reaches the receiver with minimal spreading in the near field. Three potential scenarios may arise: i) The receiver antenna aperture is smaller than the transmitter (still within the receiver's near field), ii) the receiver antenna aperture is comparable to that of the transmitter, or iii) the receiver antenna aperture is larger than that of the transmitter. If the receiver aperture is smaller, the received power decreases based on the integral formula described earlier. Maximum power reception is achieved when the receiving antenna is sufficiently large to capture the transmit beam with added minimal spreading (comparable to the transmitter). When dealing with a larger receiver, it is important to take into account the phase profile of the impinging signal, as it may lead to either constructive or destructive addition of power at the receiver. The effect is shown in Fig. 1(c) and 1(d) through the cross-sectional amplitude and phase profile, respectively, in the near field (2.5 m) of the 5 cm transmit antenna operating at 300 GHz. The receiver's near-field operation depends on its aperture size, indicated by the red circle, which could ideally be smaller, match, or exceed the transmitter's aperture size. The cross-sectional phase profile (Fig. 1(d)) shows that maximum power reception occurs with a similarly sized receiver antenna; using a smaller or larger antenna may reduce power reception.

b) Only Transmitter in Near Field: In this case, akin to the previous section, the transmitting antenna emits a broad beam within the near field. As the receiver operates in the far field, it results in a smaller aperture size compared to the transmitter, thereby decreasing the received power based on the earlier integral formula. The results are shown in Fig. 1(c) and 1(d), considering the near-field operation of the transmit antenna while the receiver antenna aperture operating in the far field is shown with a black circle (the aperture size of the receiver is back-calculated using Fraunhofer distance to ensure its far-field operation).

c) Only Receiver in Near Field: Herein, the receiver's aperture size is larger than that of the transmitter. The beam produced by the transmitter follows the propagation mechanism in the far field and spreads according to the free space path loss principle [11]. The larger receiver will intercept the beam with a different phase profile, potentially leading to a constructive or destructive addition of power. As a result, the power received by the receiver may be lower. This is illustrated in Fig. 1(e) and 1(f), where the amplitude and phase cross-sectional values are simulated at the Fraunhofer distance (5 m for 5 cm antenna at 300 GHz), ensuring transmitters' operation in the far-field region. The red circle indicates that the receiver is larger than the transmitter, ensuring that it is operating in the near-field region. Further, this phenomenon was observed in our experimental study [10], where the path loss exponent (PLE) increases with an increase in antenna aperture size, as depicted in Fig. 2. It is clear from the aforementioned three cases that the existing antenna-agonistic channel and path loss models are inadequate [3]. A revised model is necessary to effectively incorporate the observed effects.

d) Transceiver Antennas in Far Field: In this case, both antennas operate within the far field, and traditional beamforming theory remains applicable. The antenna effect can be isolated from the path loss model and channel characteristics through appropriate calibration methods. The amplitude and phase profiles are depicted in Fig. 1(e) and 1(f), respectively, exactly at the Fraunhofer distance, while the receiver is represented with a black circle having the size of a transmitter (this ensures that both antennas are operating in the far field).

IV. Effect on the Multipath Profile

Multipath profiles play a crucial role in comprehending the multipath components (MPCs) reaching the receiver from different delays and angular directions. MPCs decrease significantly in the near field due to less signal spread, which reduces non-line-of-sight (NLoS) signals reaching the receiver. Further, for a larger aperture antenna (high gain antenna), the near field extends significantly and the HPBW in the far field also decreases, resulting in reduced MPCs in both regions. Our experimental study [10] revealed that, in a conference room setup, the 40 dBi gain receiver antenna has significantly lower NLoS components compared to the 15 dBi antenna, as shown in Fig. 3(a) and 3(b), respectively. Further, with the reduced MPCs arriving at the receiver, the likelihood of the waveguide tunnel effect [17] (characterized by the constructive addition of the MPCs at the receiver) diminishes, which is reflected in the increase in the PLE n, with an increase in the antenna gain (Fig. 2). In the subsequent sections, we analyze the impact of varying antenna gains and near- and far-field effects on crucial channel metrics.

a) K-Factor: THz band communication relies highly on highly-directive antennas to combat huge path loss due to free space propagation. Therefore, it is crucial to have an estimate of the Rician K-factor, which provides the knowledge of the power at the directive component (P_D) compared to the other MPCs ($2S^2$) as a ratio and given by $K = \frac{P_D}{2S^2}$. In dB, it is represented by $10\log_{10}(K)$. This metric is crucial for determining the likelihood of a link undergoing deep fading, which decreases as the K-factor value increases. It is shown in our study (Fig. 3(c)) that the K-factor increases with an increase in antenna gain as the power at the main directive component increases as well as the number of other MPCs, and their power reduces significantly.

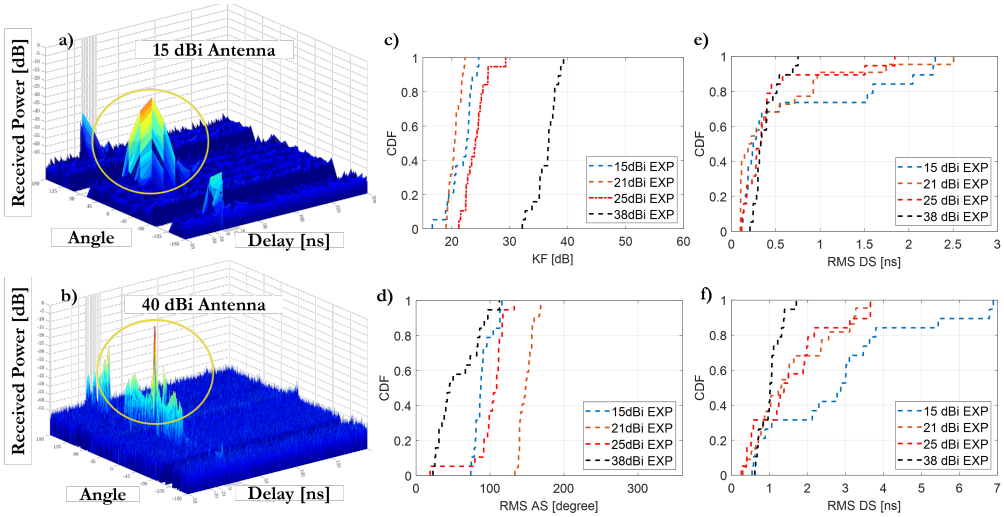

Fig. 3. Measured multipath at 140 GHz with a) 15 dBi and b) 40 dBi antennas. CDF of c) K-factor, d) angular spread, e) LoS, and f) NLoS RMS delay spreads with various receiver antennas.

b) Delay Spread: The delay spread (DS) characterizes the multipath richness of a channel. This parameter is crucial for defining the requirements of channel estimation and equalization techniques needed to mitigate inter-symbol interference (ISI). To achieve this, it is important to understand the various delayed components and their associated multipath power. The root mean square (RMS) delay spread, τ_{RMS}, is commonly used for this purpose and is calculated by $\tau_{\text{RMS}} = \sqrt{\frac{\sum_i (d_i - \hat{d})^2 \ p_i}{\sum_i p_i}}$, where d_i and p_i are the delay and received power of propagation path i, respectively, and $\hat{d}$ is the mean delay $\hat{d} = \frac{\sum_i d_i \ p_i}{\sum_i p_i}$. As the aperture or gain of an antenna increases, the extent of the near field also enlarges. Within this region, the beams propagate more gradually, leading to a reduction in the RMS DS. Additionally, in the far field, antennas characterized by high gain or directivity possess a narrower HPBW, which further diminishes the RMS DS. The CDF plot for RMS DS in both LoS and NLoS scenarios (Fig. 3(e) and 3(f), respectively) illustrates the extent of the RMS DS in a conference room setup, as shown in [10], with various antenna gains, which bolsters our discussion.

c) Angular Spread: The angular spread (AS) defines the spatial multipath richness of the wireless channel, which is crucial for understanding the possibility of establishing a communication link through an NLoS link. Mathematically, the RMS AS is given by $\text{AS}_{\text{RMS}} = \sqrt{\frac{\sum_i (\theta_i - \hat{\theta})^2 \ p_i}{\sum_i p_i}}$, where θ_i and p_i are the AoA and received power of propagation path i, respectively, and $\hat{\theta}$ is the mean AoA represented by $\hat{\theta} = \frac{\sum_i \theta_i \ p_i}{\sum_i p_i}$. In these frequency ranges, the overall AS_{RMS} is low due to the sparse nature of NLoS paths. This underscores the critical nature of establishing a reliable communication link over a 360-degree angle in the THz band. Further, a rise in antenna aperture/gain results in a reduction of AS_{RMS}, signifying a more sparse channel. This is due to minimal wave spreading in the near field and a substantial decrease in the far-field HPBW. The effect is shown in Fig. 3(d).

V. Benefits and Challenges

THz band communications, whether in the near or far field, offer a multitude of benefits but also come with some non-trivial challenges. The possibility of low-latency ultra-high data rate communications, the enabling of multiple access for millions of users, and supporting *join communications and sensing* [18], all due to the very high available bandwidths, is considered a major benefit. Another crucial benefit is that due to the use of highly directive antennas, a THz link is seen as *inherently secure* in the physical layer, which reduces the jamming possibility or channel interception. In [19], it was experimentally shown that an attempt of eavesdropping on an unencrypted sub-THz 30-meter backhaul link was extremely challenging and was only successful in detecting a faint fraction of the power of a single-frequency non-information-bearing transmitted signal. THz links in the near field offer significant advantages by enabling various wavefront engineering techniques and facilitating the spatial manipulation of THz signals [15]. This capability enhances the signal-to-interference-plus-noise ratio (SINR), which is particularly beneficial due to the directional nature of THz communications. For instance, Bessel beams can be utilized to navigate around known fixed obstacles, leveraging the inherent self-healing properties of the beam. This was experimentally shown in [20] using passive 3D-printed axicons. Orbital angular momentum (OAM) could also be utilized to achieve spatially multiplexed channels, as discussed in [21]. Going back to secure communication, the novel concept of *wavefront hopping* can achieve inherently secure THz links as explained in [15].

Despite all the promising benefits of THz communication links, we face non-trivial challenges demanding innovative solutions. As explained in the eavesdropping example, the alignment of THz links is extremely challenging, time-consuming, and even if automated, is still computationally intensive due to narrow pencil-thin beams [22]. The alignment problem becomes even more challenging in the near field as small angular mismatches could heavily alter the phase profile of

the impinged signal. Some solutions in the literature utilize intelligent reflecting surfaces (IRSs) to aid in engineering NLoS paths, especially in indoor links, where blockage and directionality are prominent problems [23]. However, current technology is not mature enough to fabricate robust and highly-tunable IRSs that have the proper elements to switch at those higher frequencies and have high efficiency and low power/reflection loss. Further, the exact location needs to be known for sophisticated wavefront technology to work, and misalignment means limited mobility schemes. Another challenge is that the extremely large bandwidths introduce the need for novel and more efficient channel estimation and equalization techniques, as it is computationally intensive to estimate the channel impulse response that contains a large number of taps/coefficients [4]. In addition, this huge bandwidth makes the beam squint effect much more prominent [24], which needs to be mitigated both in single and multicarrier systems. The design and fabrication of THz devices and hardware are very challenging due to the large bandwidths and high frequencies. This makes almost all hardware very frequency-selective, which in turn needs proper and efficient pre-distortion schemes in order to minimize the error probabilities.

VI. Conclusion

This paper describes the influence of antennas on channel models and multipath, considering the near- and far-field transitions and their benefits and challenges, particularly in light of the distinct propagation characteristics of THz waves in these regions. The study reveals that the extent of the near field is notably significant for THz systems. Moreover, it is crucial to integrate antenna-centric effects into the path loss model, as well as in the calculations of channel metrics, to obtain an accurate THz channel model. This paper underscores the significance of conducting a comprehensive experimental study of channels, taking into account various antennas at the transceiver with differing gains and apertures. It recognizes the emerging challenges associated with THz channels and presents a strategic approach to facilitate the development of THz wireless systems.

Acknowledgment

The work was supported by the U.S. AFRL NE HUB Grant 141496-23166 (FA8750-22-2-0500), the WINGS Center at SUNY Polytechnic Institute, and the U.S. National Science Foundation under Awards CNS-1955004 and CNS-2225590.

References

[1] I. F. Akyildiz, J. M. Jornet, and C. Han, "Terahertz band: Next frontier for wireless communications," *Physical Communication*, vol. 12, pp. 16–32, 2014.

[2] K. Rasilainen, T. D. Phan, M. Berg, A. Pärssinen, and P. J. Soh, "Hardware aspects of sub-THz antennas and reconfigurable intelligent surfaces for 6G communications," *IEEE Journal on Selected Areas in Communications*, vol. 41, no. 8, pp. 2530–2546, August 2023.

[3] D. Serghiou, M. Khalily, T. W. C. Brown, and R. Tafazolli, "Terahertz channel propagation phenomena, measurement techniques and modeling for 6G wireless communication applications: A survey, open challenges and future research directions," *IEEE Communications Surveys & Tutorials*, vol. 24, no. 4, pp. 1957–1996, Q4 2022.

[4] P. Sen, J. V. Siles, N. Thawdar, and J. M. Jornet, "Multi-kilometre and multi-gigabit-per-second sub-terahertz communications for wireless backhaul applications," *Nature Electronics*, vol. 6, no. 2, pp. 164–175, 2023.

[5] Y. Xing, T. S. Rappaport, and A. Ghosh, "Millimeter wave and sub-THz indoor radio propagation channel measurements, models, and comparisons in an office environment," *IEEE Communications Letters*, vol. 25, no. 10, pp. 3151–3155, 2021.

[6] P. Sen, J. Hall, M. Polese, V. Petrov, D. Bodet, F. Restuccia, T. Melodia, and J. M. Jornet, "Terahertz communications can work in rain and snow: Impact of adverse weather conditions on channels at 140 GHz," in *Proceedings of the 6th ACM Workshop on Millimeter-Wave and Terahertz Networks and Sensing Systems*, 2022, pp. 13–18.

[7] D. He, K. Guan, A. Fricke, B. Ai, R. He, Z. Zhong, A. Kasamatsu, I. Hosako, and T. Kürner, "Stochastic channel modeling for kiosk applications in the terahertz band," *IEEE Transactions on Terahertz Science and Technology*, vol. 7, no. 5, pp. 502–513, 2017.

[8] S. Ju, Y. Xing, O. Kanhere, and T. S. Rappaport, "3-D statistical indoor channel model for millimeter-wave and sub-terahertz bands," in *GLOBECOM 2020-2020 IEEE Global Communications Conference*. IEEE, 2020, pp. 1–7.

[9] J. He, Y. Chen, Y. Wang, Z. Yu, and C. Han, "Channel measurement and path-loss characterization for low-terahertz indoor scenarios," in *2021 IEEE International Conference on Communications Workshops (ICC Workshops)*. IEEE, 2021, pp. 1–6.

[10] P. Sen, S. Badran, V. Petrov, A. Singh, and J. M. Jornet, "Impact of the antenna on the sub-terahertz indoor channel characteristics: An experimental approach," in *ICC 2024 - IEEE International Conference on Communications*, 6 2024, pp. 2537–2542.

[11] C. A. Balanis, *Antenna theory: Analysis and design*. John wiley & sons, 2016.

[12] 3GPP, "Study on channel model for frequencies from 0.5 to 100 GHz (Release 17)," 3GPP, 3GPP TR 38.901 V17.0.0, March 2022.

[13] V. Petrov, J. M. Jornet, and A. Singh, "Near-field 6G networks: Why mobile terahertz communications MUST operate in the near field," in *GLOBECOM 2023-2023 IEEE Global Communications Conference*. IEEE, 2023, pp. 3983–3989.

[14] S. Amin, B. Ahmed, M. Amin, M. I. Abbasi, A. Elahi, and U. Aftab, "Establishment of boundaries for near-field, Fresnel and Fraunhofer-field regions," in *2017 IEEE Asia Pacific Microwave Conference (APMC)*. IEEE, 2017, pp. 57–60.

[15] V. Petrov, H. Guerboukha, D. M. Mittleman, and A. Singh, "Wavefront hopping: An enabler for reliable and secure near field terahertz communications in 6G and beyond," *IEEE Wireless Communications*, vol. 31, no. 1, pp. 48–55, 2024.

[16] J. Alda, "Laser and Gaussian beam propagation and transformation," *Encyclopedia of optical engineering*, vol. 999, pp. 1013–1013, 2003.

[17] H. Xu, V. Kukshya, and T. S. Rappaport, "Spatial and temporal characteristics of 60-GHz indoor channels," *IEEE Journal on selected areas in communications*, vol. 20, no. 3, pp. 620–630, 2002.

[18] A. M. Elbir, K. V. Mishra, S. Chatzinotas, and M. Bennis, "Terahertz-band integrated sensing and communications: Challenges and opportunities," *IEEE Aerospace and Electronic Systems Magazine*, 2024.

[19] Z. Shaikhanov, S. Badran, H. Guerboukha, J. M. Jornet, D. M. Mittleman, and E. W. Knightly, "MetaFly: Wireless backhaul interception via aerial wavefront manipulation," in *2024 IEEE Symposium on Security and Privacy (SP)*, 5 2024, pp. 2759–2774.

[20] I. V. Reddy, D. Bodet, A. Singh, V. Petrov, C. Liberale, and J. M. Jornet, "Ultrabroadband terahertz-band communications with self-healing Bessel beams," *Communications Engineering*, Revised, 2023.

[21] K. Miyamoto, K. Sano, T. Miyakawa, H. Niinomi, K. Toyoda, A. Vallés, and T. Omatsu, "Generation of high-quality terahertz OAM mode based on soft-aperture difference frequency generation," *Optics Express*, vol. 27, no. 22, pp. 31 840–31 849, 2019.

[22] W. Attaoui, K. Bouraqia, and E. Sabir, "Initial access & beam alignment for mmWave and terahertz communications," *IEEE Access*, vol. 10, pp. 35 363–35 397, 2022.

[23] S. Badran, A. Singh, A. Jaiswal, E. Einarsson, and J. M. Jornet, "Design and validation of a metallic reflectarray for communications at true terahertz frequencies," in *Proceedings of the 7th ACM Workshop on Millimeter-Wave and Terahertz Networks and Sensing Systems*, ser. mmNets '23, New York, NY, USA, 10 2023, p. 19–24.

[24] W. Hao, X. You, F. Zhou, Z. Chu, G. Sun, and P. Xiao, "The far-/near-field beam squint and solutions for THz intelligent reflecting surface communications," *IEEE Transactions on Vehicular Technology*, vol. 72, no. 8, pp. 10 107–10 118, 2023.